



## Full Length Article

## Formation of high-valent cobalt-oxo phthalocyanine species in a cellulose matrix for eliminating organic pollutants

Nan Li<sup>a</sup>, Wangyang Lu<sup>a,\*1</sup>, Kemei Pei<sup>b</sup>, Yuyuan Yao<sup>a</sup>, Wenxing Chen<sup>a,\*2</sup><sup>a</sup> National Engineering Lab for Textile Fiber Materials & Processing Technology (Zhejiang), Zhejiang Sci-Tech University, Hangzhou 310018, China<sup>b</sup> Department of Chemistry, Zhejiang Sci-Tech University, Hangzhou 310018, China

## ARTICLE INFO

## Article history:

Received 1 June 2014

Received in revised form 24 July 2014

Accepted 25 July 2014

Available online 4 August 2014

## Keywords:

Cellulosic fiber

Cobalt phthalocyanine

Bioinspired catalysis

Fifth ligand

Organic pollutant

## ABSTRACT

The selective elimination of recalcitrant organic pollutants in high backgrounds of complex constituents has proven a significant challenge. Inspired by the naturally occurring oxidation reactions catalyzed by metalloporphyrin-based enzymes, where the target substrates can be oxidized selectively due to the specific enzyme environment and the axial fifth ligands of metalloporphyrins, we developed a bioinspired catalytic system based on cellulosic fiber-boned cobalt phthalocyanine for capturing and oxidizing dyes by  $H_2O_2$  activation in the presence of high additive concentrations. In this system, the cellulosic fibers provided the amorphous regions, functioning as cavities in the same manner as the protein backbones of enzymes for the selective accessibility of dyes; cobalt phthalocyanine was introduced as the catalytic entity; and linear alkylbenzene sulfonate (one of the most widespread surfactants in industrial and domestic wastewater) was employed as the fifth ligand to help generate high-valent cobalt-oxo intermediates by the heterolytic cleavage of the peroxide O–O bond. According to detailed density functional theory calculations, the spin populations are predominantly located around the cobalt-oxo center, achieving an electrophilic attack on the electron-rich azo bond and the aromatic ring of the target model dyes.

© 2014 Elsevier B.V. All rights reserved.

## 1. Introduction

The growing pollution in aqueous environments, which can lead to serious and long-term threats to human health, is one of the most pervasive global problems. Most discharged recalcitrant pollutants are found at trace levels in high backgrounds of readily handled and biodegradable constituents [1,2]. The elimination of these microcontaminants has always been a great challenge in water purification and has garnered increased concern worldwide [3–7]. Although many oxidation methods have been developed for eliminating organic pollutants [8–10], target pollutants are often inefficiently oxidized in the presence of organic and inorganic matrices that are a thousand to a million fold more abundant [1]. Thus, a desirable oxidation system for removing recalcitrant pollutants must be shielded from the interference of external

complicated constituents or employ these constituents to promote the elimination of the target contaminants.

Coordination complex catalysts such as metalloporphyrins (MPs) and metallophthalocyanines (MPcs) have been extensively studied as mimic enzyme catalysts for activating  $O_2$ ,  $H_2O_2$  or other peroxides to facilitate the elimination of organic pollutants [11–15]. Among the reactions using  $H_2O_2$  as the oxidant, the generation of hydroxyl radicals ( $\bullet OH$ ) and metal-oxo-based intermediates, corresponding to the homolytic and heterolytic cleavage of the peroxide O–O bond [16–18], have proven most effective in oxidizing organic contaminants. However, in high backgrounds of complicated constituents, both of these active species inevitably react with the high-concentration and easily handled constituents or the free coordination catalysts in homogeneous systems, leading to the inefficient oxidation of low-concentration recalcitrant contaminants [19] or the oxidative destruction of the catalysts themselves [16]. As a potent H-atom abstractor,  $\bullet OH$  is theoretically able to move freely and react with all organic matter involving high-concentration constituents, as the O–H bond of water is stronger than nearly all C–H bonds [20]. In contrast, the supported coordination complexes may exhibit good stability toward the autoxidation of

<sup>\*</sup> Corresponding authors. Tel./fax: +86 571 8684 3611.E-mail addresses: [luwy@zstu.edu.cn](mailto:luwy@zstu.edu.cn) (W. Lu), [wxchen@zstu.edu.cn](mailto:wxchen@zstu.edu.cn) (W. Chen).<sup>1</sup> Tel./fax: +86 571 86843611.<sup>2</sup> Tel./fax: +86 571 86843611.

catalytic entities when the reactions are dominated by metal-oxo based intermediates, as the coordination complex in this case has been covalently anchored to the support, thereby minimizing the possibility of autoxidation. Therefore, effective strategies for designing catalytic systems based on coordination complexes should control the reaction channels of  $\text{H}_2\text{O}_2$  activation without generating  $\bullet\text{OH}$  [20,21]; the heterolytic cleavage of the O–O bond is more desirable for the catalytic systems of coordination complexes.

Notably, in most enzymatic reactions, the target substrate is selectively captured in a region that contains active sites, followed by the rapid oxidation of the substrate. The catalytic entity, cofactors and protein backbone represent the heart of enzyme-catalyzed systems. In such systems, the protein backbone provides the steric environment for the substrate to become attached to the active sites and protects the active sites against external interference, while cofactors (such as the axial ligands in metalloporphyrin-based enzymatic reactions) determine the reaction channels [22–24]. For example, horseradish peroxidase presents peroxidase-like activity in the presence of the imidazole ligand of a histidine residue, while catalase presents catalase-like activity when presented with the phenolate ligand of a tyrosine residue. Generally, the high oxidation states of the central transition metal ions tend to become stabilized in MPs, while the phthalocyanine ligand tends to stabilize the lower oxidation states of metals, implying that high oxidation states of MPcs have stronger oxidizing abilities than those of MPs [18]. Both high-valent metal-oxo species and  $\bullet\text{OH}$  have been previously reported in MPcs-activated  $\text{H}_2\text{O}_2$  systems. However, few studies have focused on the precise control of O–O bond cleavage by introducing the fifth ligand into such a system.

In the present paper, we report a bioinspired strategy for removing organic contaminants in high backgrounds of complicated constituents as exemplified by the elimination of recalcitrant dyes from dyeing effluents, of which several billion tons are produced annually, containing massive amounts of organic and inorganic additives (concentrations 100–1000 times higher than those of dyes). These additives are necessary to improve dye penetration into fibers during the dyeing process through hydrophobic and electrostatic interactions [25]. Therefore, the degradation of dye effluents remains a significant problem and has recently attracted a great deal of attention [26–29]. In this work, a bioinspired catalytic system based on cellulosic fiber-bonded cobalt phthalocyanine (CoPc-F, Scheme S1A) was developed to eliminate dyes by  $\text{H}_2\text{O}_2$  activation, using the enzyme mimic catalyst cobalt phthalocyanine (CoPc) as the catalytic entity. Compared with iron phthalocyanine, CoPc derivatives have better chemical stability and are more affordable [30]. Linear alkylbenzene sulfonate (one of the most widespread surfactants in dye effluents) was employed as the fifth ligand to control the reaction channel of O–O bond cleavage. As an important applied form of cellulose (the most abundant biomaterial on earth), cellulosic fibers could play the role of the protein backbones in enzymes, as their swelling properties facilitate dye penetration and their amorphous regions function as cavities that introduce catalytic entities and cofactors to generate active sites, thereby creating an enzyme-like environment with regioselectivity for organic dyes. The catalytic oxidation of azo dyes (accounting for 60%–70% of all organic dye production worldwide [31,32]) was conducted in the presence of several typical additives with high concentrations. The generated active species and oxidation pathway of C.I. Acid Red 1 (AR1, employed as the major model) are presented as determined through in situ electron paramagnetic resonance (EPR), density functional theory (DFT) calculations and ultra-performance liquid chromatography/high-definition mass spectrometry.

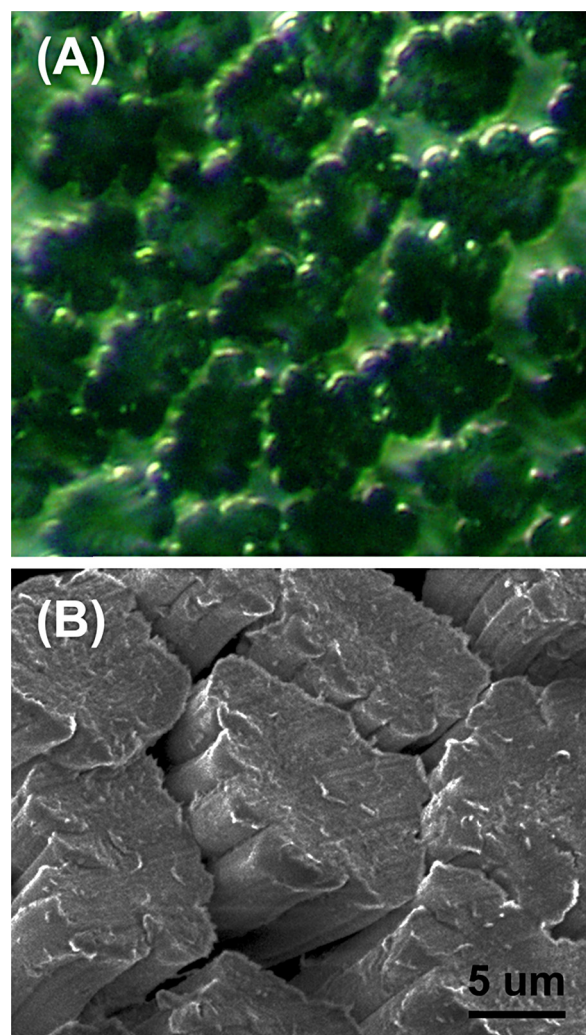


Fig. 1. Photomicrograph (A) and SEM (B) of the CoPc-F cross section.

## 2. Experimental

### 2.1. Materials

Cellulosic fibers were supplied by Fulida Co., Ltd. (Zhejiang, China). AR1 and C.I. Acid Orange 7 (AO7) were purchased from Acros and were used without further purification. C.I. Reactive Red 2 (RR2) and C.I. Reactive Blue 19 (RB19) were commercial compounds and were used without further purification. Sodium linear-dodecylbenzenesulfonate (LAS) was obtained from Tianjin Kemiou Chemical Reagent Co., Ltd. The spin-trap reagent, 5,5-dimethyl-pyrroline-oxide (DMPO), was reagent grade and was purchased from Tokyo Chemical Industry Co., Ltd. Poly(ethylene glycol) (PEG,  $M_w = 1000$ ), urea and  $\text{H}_2\text{O}_2$  (9.7 M) were purchased from Sinopharm Chemical Reagent Co., Ltd. CoPc-F was synthesized by covalently immobilizing cobalt tetra(2,4-dichloro-1,3,5-triazine)aminophthalocyanine to the cellulosic fibers according to previously described methods [30]. Water-soluble cobalt tetra(*N*-carboxylic)aminophthalocyanine (CoMPc, Scheme S1B) was synthesized by modifying cobalt tetraaminophthalocyanine with maleic anhydride according to a previously reported method [33]. The content of CoPc in CoPc-F was calculated to be 7.2  $\mu\text{mol/g}$  using an atomic absorption spectrometer (Thermo Solar M6). As seen in the photomicrograph cross section of CoPc-F (Fig. 1A, obtained using an Olympus 1X71 at  $\times 400$  magnification), the green CoPc was loaded uniformly to the interiors of the cellulose fibers. The

diameter of CoPc-F is approximately  $10\text{ }\mu\text{m}$  according to the scanning electron microscopy (SEM, JEOL JSM-5610V) image of the cross section of CoPc-F in Fig. 1B.

## 2.2. Catalytic oxidation experiment

The catalytic oxidation of AR1 ( $5 \times 10^{-5}$  mol/L) and three other primary color dyes (RR2, RB19 and AO7) was conducted using CoPc-F (1.25 g/L, containing  $9.0\text{ }\mu\text{mol/L}$  CoPc) and  $\text{H}_2\text{O}_2$  ( $1.0 \times 10^{-2}$  mol/L) at  $50^\circ\text{C}$  with an LAS concentration of  $1.4 \times 10^{-3}$  mol/L. The catalytic oxidation of AR1 ( $5 \times 10^{-5}$  mol/L) in a typical Fenton ( $\text{Fe}^{2+}/\text{H}_2\text{O}_2$ , pH 3) system was conducted using  $\text{Fe}^{2+}$  ( $9.0\text{ }\mu\text{mol/L}$ ) and  $\text{H}_2\text{O}_2$  ( $1.0 \times 10^{-2}$  mol/L) at  $50^\circ\text{C}$  in the presence of urea ( $0.1\text{ mol/L}$ ) or PEG ( $[\text{CH}_2\text{CH}_2\text{O}] = 0.1\text{ mol/L}$ ). The homogeneous contrast experiment maintained equal molar concentrations of CoMPc and CoPc in CoPc-F. The reaction solutions were adjusted to the desired pH value using  $\text{HClO}_4$  ( $0.1\text{ mol/L}$ ) and  $\text{NaOH}$  ( $0.1\text{ mol/L}$ ). The reaction was initiated when  $\text{H}_2\text{O}_2$  was added into the solution. The continuous cycle experiments were performed eight times. For each run, a known concentration of AR1 was added into the reaction system to maintain the initial concentration of  $5.0 \times 10^{-5}$  mol/L, and  $\text{H}_2\text{O}_2$  ( $1.0 \times 10^{-2}$  mol/L) was added every cycle.

## 2.3. Analysis

Ultra-performance liquid chromatography (UPLC, Acquity BEH C18 column ( $1.7\text{ }\mu\text{m}$ ,  $2.1 \times 50\text{ mm}$ ), Waters) was employed for immediate analysis at the given time points. Detection of AR1 was accomplished using a photodiode array detector (PDA) set at  $311.7\text{ nm}$ . The binary system phases were (A) water with an ion pairing agent ( $50\text{ mM}$  ammonium acetate and  $2\text{ mM}$  tetrabutyl ammonium bromide) and (B) acetonitrile; the eluent consisted of A and B ( $1:1$ , v/v) with a flow rate of  $0.4\text{ mL/min}$ . We attempted to detect the oxidative intermediates of AR1 in the presence of CoPc-F, LAS and  $\text{H}_2\text{O}_2$  using UPLC/Synapt G2-S HDMS (Waters) after 15 and 60 min of reaction time (Fig. S8 and Table S1, respectively). Chromatographic separation was conducted with a BEH C18 column ( $1.7\text{ }\mu\text{m}$ ,  $2.1 \times 100\text{ mm}$ ) using mobile phases A (water) and B (acetonitrile). The gradient began with  $95\%$  A at 0 min, where it was held for 0.5 min, followed by a decrease to  $80\%$  A at 4 min. The gradient reached  $50\%$  A at 5 min, and in the next 2 min it remained at  $10\%$  A, finally reaching  $90\%$  A at 12.1 min. The flow rate was  $0.5\text{ mL/min}$ , and the column oven temperature was set at  $30^\circ\text{C}$ . The parameters for the Synapt G2-S HDMS analyses were as follows: ESI negative ion mode, lockmass correction of leucine enkephaline (LE, Tyr-Gly-Gly-Phe-Leu,  $m/z$  554.2615), and the scan range was set to  $50\text{--}1200\text{ m/z}$ . A Bruker A300 spectrometer was used to record the EPR signals of DMPO at  $20^\circ\text{C}$  with the following settings: center field,  $3517.5\text{ G}$ ; sweep width,  $55\text{ G}$ ; microwave frequency,  $9.882\text{ GHz}$ ; modulation frequency,  $100\text{ kHz}$ ; power,  $20\text{ mW}$ . The signals of high-valent cobalt-oxo phthalocyanine species and other cobalt complexes were measured at  $20^\circ\text{C}$  with the following settings: center field,  $3400\text{ G}$ ; sweep width,  $2000\text{ G}$ ; microwave frequency,  $9.877\text{ GHz}$ ; modulation frequency,  $100\text{ kHz}$ ; power,  $20\text{ mW}$ . Before EPR analysis, the CoPc-F were immersed into the reaction solution (containing LAS and  $\text{H}_2\text{O}_2$ ) for 1 min and were then quickly removed and wrung out. The DFT calculations presented in this work were performed using the Gaussian program [34].

## 3. Results and discussion

### 3.1. Catalytic oxidation of dyes

In the present study, we chose AR1 as the main model contaminant for investigating the performance of a bioinspired catalytic

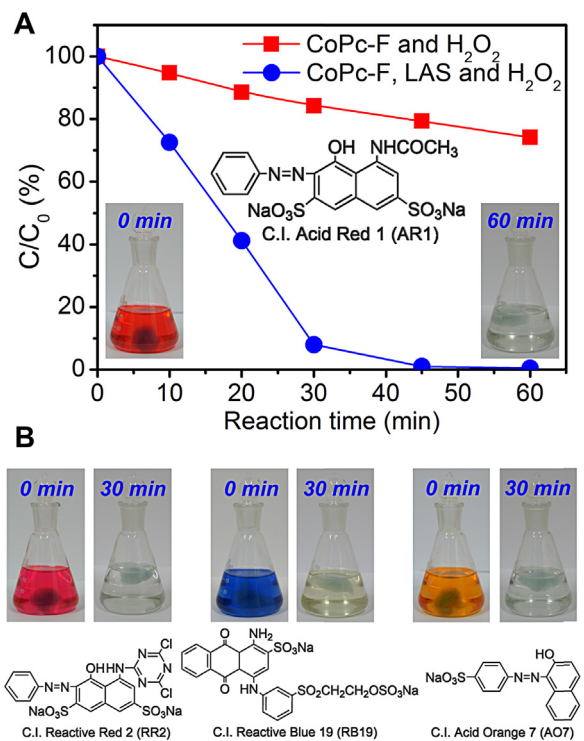


**Fig. 2.** (A) Catalytic oxidation of AR1 at pH 10 by CoPc-F under different conditions and the digital picture of the AR1 solution before and after the reaction in the presence of CoPc-F,  $\text{H}_2\text{O}_2$  and LAS, where  $C$  represents the dye concentration at different reaction times and  $C_0$  represents the initial concentration; (B) the digital picture of three primary color dyes (RR2, RB19 and AO7) before and after oxidation in the presence of CoPc-F,  $\text{H}_2\text{O}_2$  and LAS.

system based on CoPc-F. As shown in Fig. 2A, a dramatic decline of AR1 concentration was achieved in the presence of LAS and  $\text{H}_2\text{O}_2$ , and the color of the solution changed from red to colorless after 60 min. However, this high activity was not observed in the absence of LAS (Fig. 2A) or in other comparative systems (Fig. S1). Moreover, in comparison with the results of a previous study [30], greatly enhanced catalytic activity was achieved under alkaline conditions (pH 10) when LAS was present. During the catalytic oxidation of AR1, the concentration of LAS declined slightly and reached equilibrium quickly (Fig. S2). This result may have been caused by an interaction between CoPc-F and LAS. The presence of LAS significantly increased the removal efficiency of AR1. This catalytic system also efficiently eliminated other azo dyes with different colors and structures under the same conditions with LAS and  $\text{H}_2\text{O}_2$  (Fig. 2B). More importantly, this bioinspired catalytic system was effective at neutral pH (Fig. S3).

Massive amounts of additives such as urea and PEG-containing compounds are necessary to promote dye penetration into fibers during the dyeing process [35], causing some difficulties for the highly effective oxidation of dyes in practical effluents [19]. In this work, the oxidation of AR1 in the bioinspired catalytic system was conducted in the presence of typical constituents, including urea and PEG. As shown in Fig. 3A, the removal efficiency for the target contaminant AR1 in the CoPc-F/LAS catalytic system was significantly improved in high backgrounds (thousand fold more abundant) of urea and PEG. Urea acts as a swelling agent for textile dyeing and can break the intermolecular bonds in cellulosic fibers by producing internal stresses [36], thereby expanding the amorphous region of cellulosic fibers [37,38]. Similarly, PEG can also break the intermolecular hydrogen bonds of the cellulose chain, thereby promoting the penetration of dyes. However, in a typical Fenton ( $\text{Fe}^{2+}$  and  $\text{H}_2\text{O}_2$ , pH 3) system, the introduction

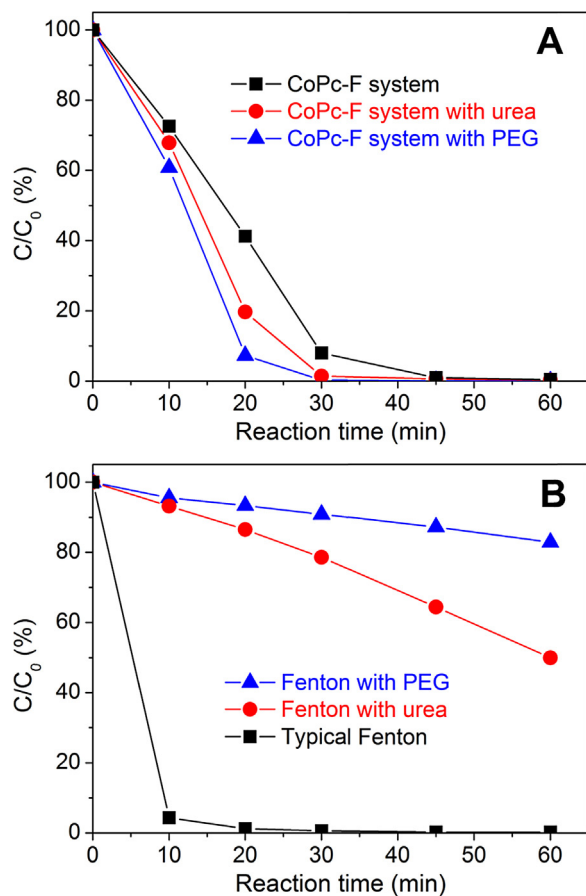


**Fig. 3.** Oxidative elimination of AR1 ( $5 \times 10^{-5}$  mol/L) by the CoPc-F/H<sub>2</sub>O<sub>2</sub> system with LAS (A) or by a typical Fenton (Fe<sup>2+</sup> and H<sub>2</sub>O<sub>2</sub>) system (B) in high backgrounds of urea (0.1 mol/L) and PEG ( $[\text{CH}_2\text{CH}_2\text{O}] = 0.1$  mol/L).

of urea and PEG dramatically reduced the removal efficiency of the target AR1 (Fig. 3B), as the high-concentration and biodegradable urea and PEG could more easily react with free •OH in the reaction kinetics. Therefore, the bioinspired catalytic system (containing CoPc-F and LAS) transformed the negative effects of the external constituents that occurred in a typical •OH-dominated Fenton reaction into positive factors for the oxidation of recalcitrant dyes.

### 3.2. Mechanism and pathway

To demonstrate the catalytic mechanism of this bioinspired catalytic system, EPR spin-trapping experiments with DMPO were conducted. Nearly no DMPO-•OH signals were observed with LAS, while a DMPO-•OH signal was detected without LAS (Fig. 4A). This result confirmed the existence of a non-hydroxyl radical process in the presence of LAS. To further determine the real active species, we conducted an in situ EPR experiment to detect the active intermediates of CoPc-F. An obvious EPR signal at  $g_{\text{eff}} = 2.099$  was observed at room temperature after CoPc-F was immersed into the reaction solution (containing LAS and H<sub>2</sub>O<sub>2</sub>) for a short time and then quickly wrung out (Fig. 4B). However, no EPR signal was observed in the absence of LAS. To aid in the assignment of the above resulting species, we investigated the EPR spectra of two common cobalt complexes,  $[\text{Co}(\text{CN})_6]^{4-}$  and  $[\text{Co}(\text{en})_3]^{2+}$ , which have relatively low standard reduction potentials ( $-0.8$  V and  $-0.2$  V, respectively) [39] and are easily oxidized into high-valent cobalt complexes. When the  $[\text{Co}(\text{CN})_6]^{4-}$  solution was first exposed to O<sub>2</sub>, the observed  $g_{\text{eff}} = 2.14$  and  $g_{\text{eff}} = 2.017$  signals (Fig. 5) could be assigned to Co<sup>II</sup>

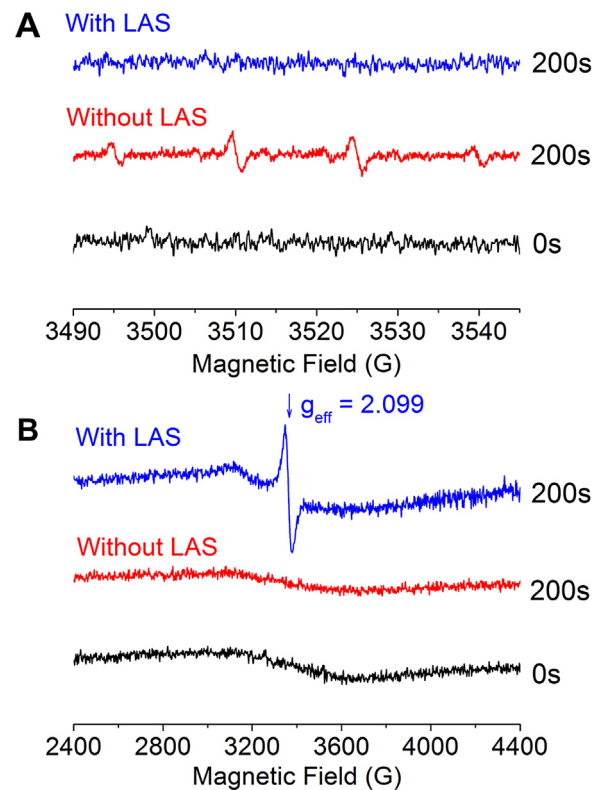


**Fig. 4.** (A) DMPO spin-trapping EPR spectra in AR1 ( $5 \times 10^{-5}$  mol/L) aqueous solution in the presence of CoPc-F (1.25 g/L, containing  $9.0 \times 10^{-6}$  mol/L CoPc) with or without LAS ( $1.4 \times 10^{-3}$  mol/L),  $[\text{H}_2\text{O}_2]_0 = 1.0 \times 10^{-2}$  mol/L,  $[\text{DMPO}] = 5.0 \times 10^{-3}$  mol/L; (B) in situ X-band EPR spectra of the active intermediates in CoPc-F with or without LAS. Experimental data recorded at 20 °C.

and Co<sup>IV</sup> species, respectively, as the partial  $[\text{Co}(\text{CN})_6]^{4-}$  was oxidized and CN<sup>-</sup> is a strong-field ligand that generates a low-spin Co<sup>III</sup> site exhibiting an EPR-silent configuration. As oxidation proceeded, the observed Co<sup>II</sup> signal disappeared, and the Co<sup>IV</sup> signal increased. The same Co<sup>IV</sup> species signal was also observed in the system with  $[\text{Co}(\text{CN})_6]^{4-}$  and H<sub>2</sub>O<sub>2</sub>. In addition, a similar result arose in the oxidation of  $[\text{Co}(\text{en})_3]^{2+}$  with H<sub>2</sub>O<sub>2</sub>, in which the  $g_{\text{eff}} = 2.03$  signal was assigned to Co<sup>IV</sup> species (Fig. 6). It should be noted the high-valent iron-oxo phthalocyanine cation radical and the Co<sup>III</sup> π-cation radical have previously been reported to yield extremely narrow signals at  $g = 2.01$  (at 120 K) and  $g = 2.0038$  (at 25 K), respectively [40,41], which are close to the  $g$ -value of a free electron

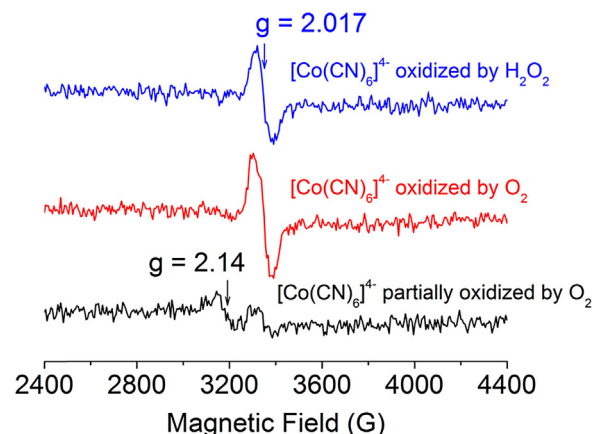


**Fig. 5.** X-band EPR spectra of the oxidative intermediates of  $[\text{Co}(\text{CN})_6]^{4-}$  by O<sub>2</sub> and H<sub>2</sub>O<sub>2</sub>. Experimental data recorded at 20 °C.

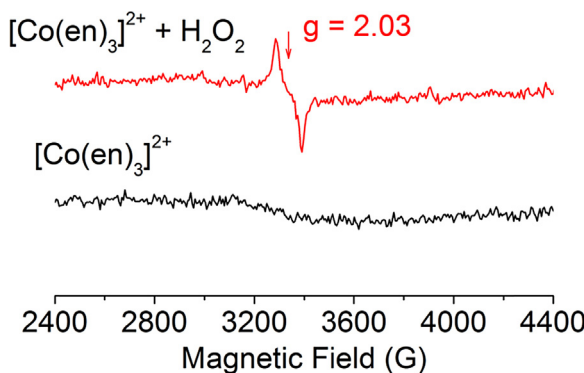


**Fig. 6.** X-band EPR spectra of the oxidative intermediates of  $[\text{Co}(\text{en})_3]^{2+}$  by  $\text{H}_2\text{O}_2$ . Experimental data recorded at 20 °C.

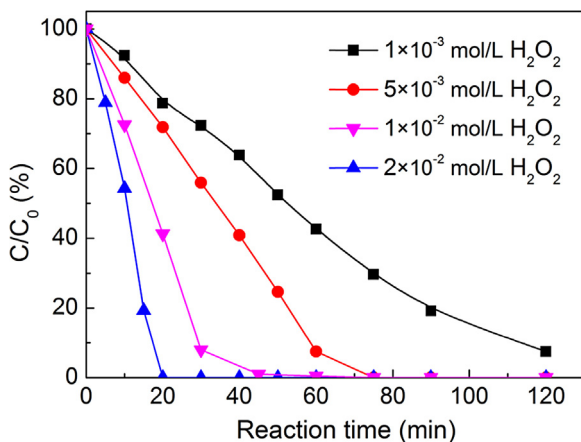


**Fig. 7.** Effects of  $\text{H}_2\text{O}_2$  concentration on the oxidative elimination of AR1 ( $5 \times 10^{-5}$  mol/L) in the presence of CoPc-F (1.25 g/L, containing  $9.0 \times 10^{-6}$  mol/L CoPc) and LAS ( $1.4 \times 10^{-3}$  mol/L) (50 °C, pH 10).

( $g_{\text{eff}} = 2.0023$ ). Because the cobalt ion of CoPc bonds with the strong-field tetrapyrrolic ligands, we are confident that the  $\text{Co}^{III}$  sites in CoPc-F are low-spin and that the signal observed at  $g_{\text{eff}} = 2.099$  provides evidence for assigning the resonance to  $\text{Co}^{IV}$  species ( $S = 1/2$ ).

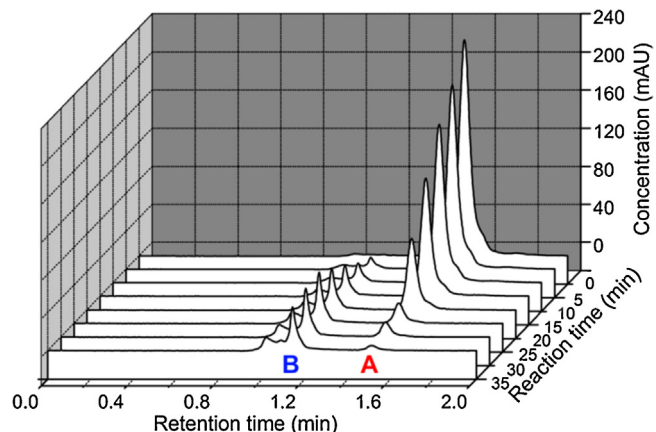


**Fig. 9.** Temporal UPLC spectra profiles during the catalytic oxidation of AR1 ( $5 \times 10^{-5}$  mol/L) obtained from UPLC-PDA.  $[\text{CoPc-F}] = 1.25 \text{ g/L}$  (containing  $9.0 \times 10^{-6}$  mol/L CoPc),  $[\text{H}_2\text{O}_2]_0 = 1.0 \times 10^{-2}$  mol/L,  $[\text{LAS}] = 1.4 \times 10^{-3}$  mol/L, 50 °C, pH 10, detection wavelength: 311.7 nm.

Thus the high-valent cobalt-oxo ( $\text{PcCo}^{IV}=\text{O}$ ) intermediates were identified as the major active species. These active species exhibited high reactivity for AR1 oxidation even under low concentrations of  $\text{H}_2\text{O}_2$  (1 mM), as shown in Fig. 7, and the utilization of  $\text{H}_2\text{O}_2$  was greatly improved, indicating that this non-radical reaction system could significantly reduce the disproportionate amount of  $\text{H}_2\text{O}_2$  present in some  $\bullet\text{OH}$ -involving reaction systems.

Promisingly, most high-valent metal-oxo species have been detected at very low temperatures [40,41]; the high oxidation state  $\text{PcCo}^{IV}=\text{O}$  was measured at room temperature, indicating that high oxidation state intermediates can be anchored in the cellulose matrix without autoxidation. This speculation was confirmed by the cyclic experiments, in which the catalytic fibers exhibited high catalytic activity to eliminate AR1 in each successive cycle (Fig. S4). No free cobalt ions or CoPc were detected in the aqueous solution by the atomic absorption spectrometer after the cyclic experiments, suggesting that the catalytic entity of CoPc in the cellulosic fibers has excellent persistence and stability. In contrast, the EPR spectrum of the homogeneous CoMPc system with LAS

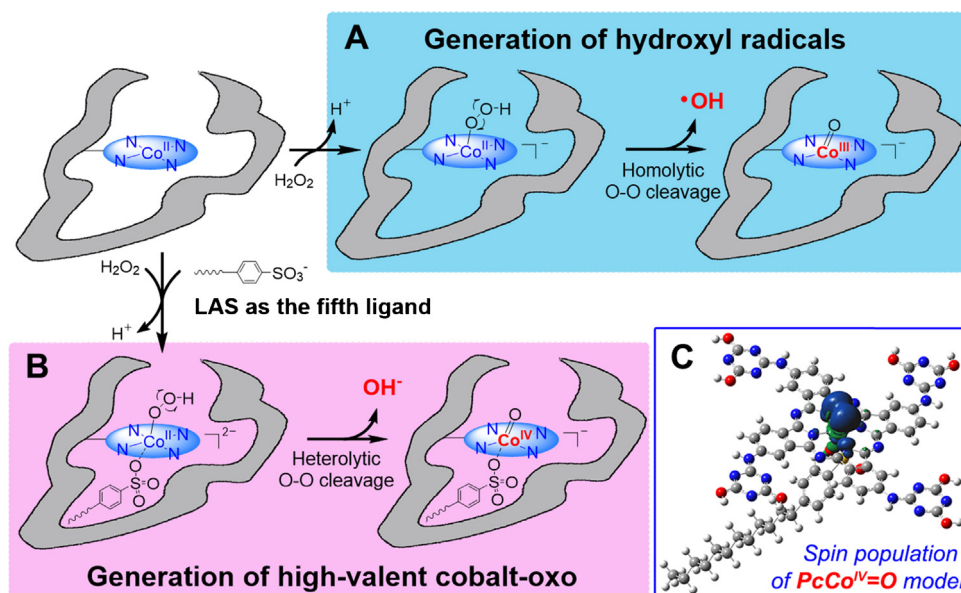


**Fig. 8.** Possible pathways for the formation of active species in CoPc-F-activated  $\text{H}_2\text{O}_2$  systems. (A) Generation of hydroxyl radicals without LAS by the homolytic cleavage of the peroxide O–O bond; (B) generation of high-valent cobalt-oxo with LAS by the heterolytic cleavage of the peroxide O–O bond; (C) calculated spin population for the  $\text{PcCo}^{IV}=\text{O}$  model of CoPc-F in the presence of LAS.

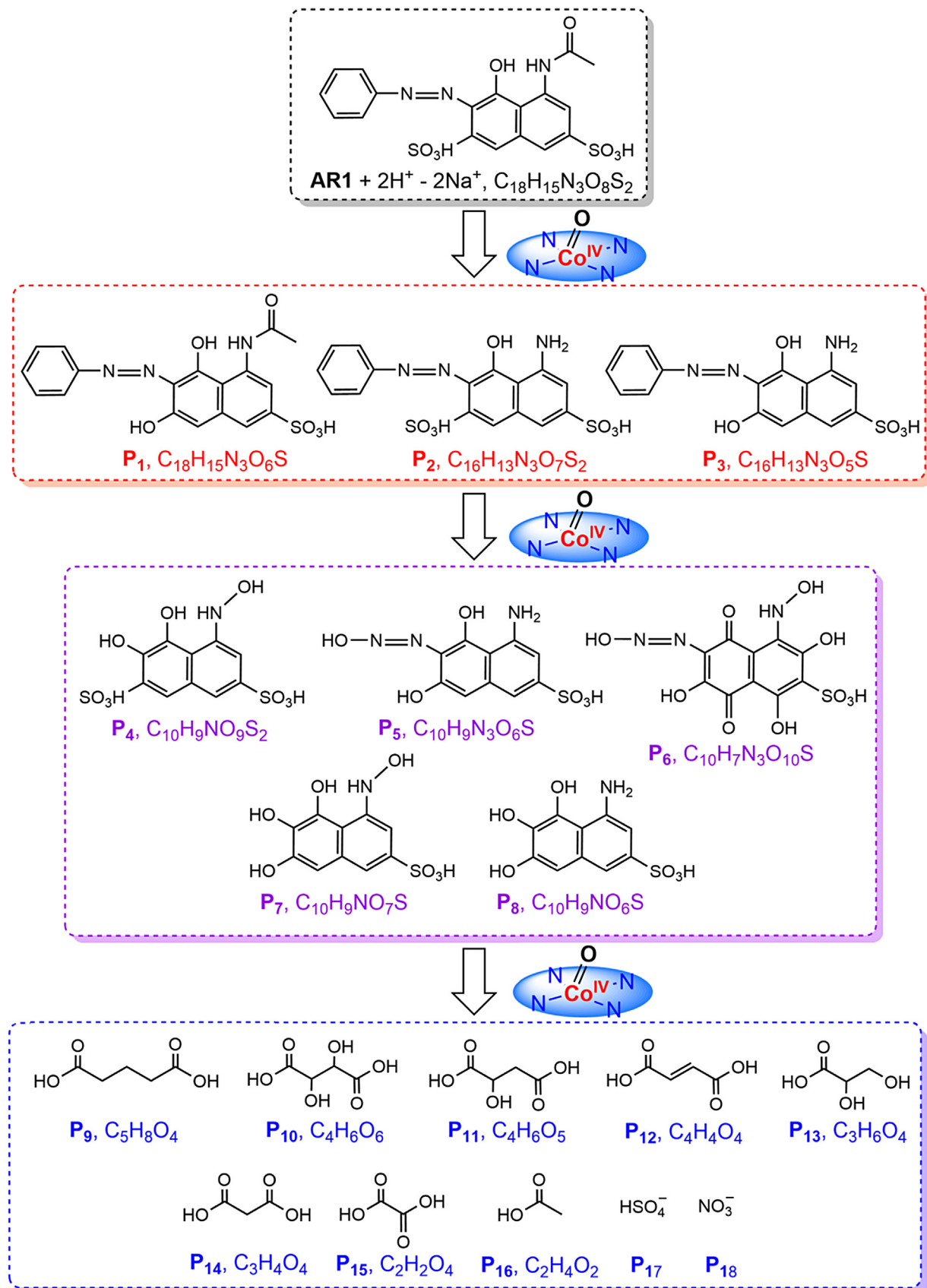


**Fig. 10.** Possible pathway for the catalytic oxidation of AR1 in the presence of CoPc-F, LAS and H<sub>2</sub>O<sub>2</sub>. (P<sub>1</sub>–P<sub>18</sub> were detected by UPLC Synapt G2-S HDMS in the negative ion mode.).

and  $\text{H}_2\text{O}_2$  did not exhibit any signal attributable to  $\text{Co}^{\text{IV}}$  species (Fig. S5). This result may have been due to the rapid reaction of the generated free species with the substrates or the catalytic entities themselves. Although the homogeneous system achieved enhanced AR1 removal due to the introduction of LAS (Fig. S6), almost half of the CoMPc was oxidized after 60 min of reaction (Fig. S7). Therefore, both  $\bullet\text{OH}$  and metal-oxo-based intermediates inevitably come into contact with the high backgrounds of complex constituents or themselves in homogeneous catalytic systems due to their free movement, thus leading to the inefficient oxidation of the target contaminants or the autoxidation of catalytic entity.

The homolytic and heterolytic cleavage of the peroxide O–O bond are generally in competition [18,42]. Corresponding to the obvious DMPO- $\bullet\text{OH}$  signal in the EPR data for the CoPc-F/ $\text{H}_2\text{O}_2$  system without LAS (Fig. 3A), the homolytic cleavage of the peroxide O–O bond is the pathway that forms  $\bullet\text{OH}$  and low-spin  $\text{Co}^{\text{III}}$  intermediates (Fig. 8A); this conclusion was verified by in situ EPR experiments for CoPc-F in the absence of LAS (Fig. 4B). The coordination behavior of divalent metal ions in the first transition series toward the  $\text{SO}_3^-$  group of aryl-sulfonates does not occur in an aqueous solution, in which the divalent metal ions are coordinated by six water molecules. However, when these ions (such as  $\text{Co}^{2+}$ ,  $\text{Ni}^{2+}$ , etc.) lie on an inversion center coordinated by N-containing ligands, the O atom from  $\text{SO}_3^-$  displays a weak coordination with the metal ions at their remaining coordination sites [43–46]. Therefore, CoPc (covalently anchored on the fibers) is coordinated axially by  $\text{OOH}^-$  and the O atom of  $\text{SO}_3^-$  from LAS to form the hydroperoxo complex (Fig. 8B). The heterolytic cleavage of the peroxide O–O bond is the more likely reaction, as  $\text{H}_2\text{O}_2$  is a single oxygen atom donor [47] and LAS (acting as the fifth ligand) could provide a “push” effect, resulting in  $\text{PcCo}^{\text{IV}}=\text{O}$  generation (Fig. 8B).

We also modeled the reaction process by DFT with the B3LYP/6-31G method. The DFT calculations showed that the Co–O ( $\text{SO}_3^-$ ) bond (1.997 Å) was longer than the cobalt(IV)-oxo bond (1.800 Å) in the simplified model of CoPc-F (Scheme S1C) with LAS and  $\text{H}_2\text{O}_2$ , indicating that the LAS ligand exerts a sizable influence on  $\text{PcCo}^{\text{IV}}=\text{O}$  formation by the heterolytic cleavage of the peroxide O–O bond. According to the detailed DFT calculations, the spin populations are predominantly located around the cobalt-oxo center of  $\text{PcCo}^{\text{IV}}=\text{O}$  (Fig. 8C), which allows the active species to achieve the electrophilic addition of an azo bond or electrophilic aromatic substitution on the azo substrate. As shown in Fig. 9, the peak (A) of AR1 gradually declined, while a new naphthalene peak (B) with a retention time of ~1.144 min appeared rapidly and then decreased after 25 min of reaction, indicating that some intermediates with naphthalene structures were formed and could be further oxidized via ring opening. To further identify the possible products, the oxidative intermediates of AR1 in this catalytic system were examined by UPLC Synapt G2-S HDMS in the negative ion mode after 15 and 60 min of reaction time, as shown in Fig. S8 and Table S1. The possible mechanism for the oxidation of AR1 in this bioinspired catalytic system is shown in Fig. 10. First, the oxygen atoms from the highly reactive  $\text{PcCo}^{\text{IV}}=\text{O}$  species could be inserted into the electron-rich azo bond and aromatic ring of AR1 to produce deacetylated and/or desulfonated intermediates (P<sub>1</sub>–P<sub>3</sub>). Secondly, several naphthalene ring-containing compounds (P<sub>4</sub>–P<sub>8</sub>) were formed, which could be confirmed by the results in Fig. 9. Finally, several biodegradable low-molecular-weight organic acids (P<sub>9</sub>–P<sub>16</sub>) and inorganic salts such as  $\text{HSO}_4^-$  (P<sub>17</sub>) and  $\text{NO}_3^-$  (P<sub>18</sub>) were obtained due to aromatic ring-opening oxidation.

## 4. Conclusion

In summary, we constructed a bioinspired catalytic system using cellulosic fiber-bonded CoPc to eliminate dyes in the presence

of  $\text{H}_2\text{O}_2$ . LAS acts as the fifth ligand, promoting the heterolytic cleavage of the O–O bond to generate active  $\text{PcCo}^{\text{IV}}=\text{O}$  species, which were detected by in situ EPR experiments and could be isolated from each other by anchoring on fibers to minimize the autoxidation of catalytic entities and consumption due to reactions with other complex constituents. This work provides new insight into the elimination of recalcitrant dyes, as well as that of low-concentration contaminants in high backgrounds of complex constituents. However, desirable methods for treating wastewater with recalcitrant contaminants and high concentrations of readily handled constituents should combine powerful advanced oxidation processes and inexpensive biotreatments. The biodegradable products of recalcitrant contaminants and other highly concentrated, readily handled constituents could be treated easily by biological processes. Future studies should focus on eliminating a wide range of microcontaminants by designing appropriate reaction systems with excellent capture capability and bonded-active sites.

## Author Contributions

The manuscript was written through contributions of all authors. All authors have given approval to the final version of the manuscript.

## Conflicts of Interest

The authors declare no competing financial interest.

## Acknowledgment

This work was supported by the National Natural Science Foundation of China (No. 51133006 and 51103133), Textile Vision Science & Education Fund, 521 Talent Project of ZSTU, and Zhejiang Provincial Natural Science Foundation of China (No. LY14E030013 and LY14E030015). We are grateful to Minxin Meng for his technical support of the UPLC Synapt G2-S HDMS data.

## Appendix A. Supplementary data

Supplementary data associated with this article can be found, in the online version, at <http://dx.doi.org/10.1016/j.apcatb.2014.07.056>.

## References

- [1] R.P. Schwarzenbach, B.I. Escher, K. Fenner, T.B. Hofstetter, C.A. Johnson, U. Gunten, B. Wehrli, *Science* 313 (2006) 1072–1077.
- [2] M.A. Shannon, P.W. Elimelech, M. Bohn, J.G. Georgiadis, B.J. Mariñas, A.M. Mayes, *Nature* 452 (2008) 301–310.
- [3] L. Hernández-Leal, H. Temmink, G. Zeeman, C.J.N. Buisman, *Water Res.* 45 (2011) 2887–2896.
- [4] D.L. Sedlak, J.L. Schnoor, *Environ. Sci. Technol.* 47 (2013) 5517–5517.
- [5] J.T. Jasper, D.L. Sedlak, *Environ. Sci. Technol.* 47 (2013) 10781–10790.
- [6] I.A. Katsygiannis, S. Canonica, U. von Gunten, *Water Res.* 45 (2011) 3811–3822.
- [7] J. Fang, Y. Fu, C. Shang, *Environ. Sci. Technol.* 48 (2014) 1859–1868.
- [8] A. Lv, C. Hu, Y. Nie, J. Qu, *Appl. Catal. B: Environ.* 117–118 (2014) 246–252.
- [9] M. Canals, R. Gonzalez-Olmos, M. Costas, A. Company, *Environ. Sci. Technol.* 47 (2013) 9918–9927.
- [10] N. Patel, R. Jaiswal, T. Warang, G. Scarduelli, A. Dashora, B.L. Ahuja, D.C. Kothari, A. Miottello, *Appl. Catal. B: Environ.* 150–151 (2014) 74–81.
- [11] J.K. Joseph, S.L. Jain, B. Sain, *Ind. Eng. Chem. Res.* 49 (2010) 6674–6677.
- [12] X. Tao, W. Ma, T. Zhang, J. Zhao, *Angew. Chem. Int. Ed.* 40 (2001) 3014–3016.
- [13] W. Lu, W. Chen, N. Li, M. Xu, Y. Yao, *Appl. Catal. B: Environ.* 87 (2009) 146–151.
- [14] M. Gao, N. Li, W. Lu, W. Chen, *Appl. Catal. B: Environ.* 147 (2014) 805–812.
- [15] Z. Huang, H. Bao, Y. Yao, W. Lu, W. Chen, *Appl. Catal. B: Environ.* 154–155 (2014) 36–43.
- [16] W.C. Ellis, C.T. Tran, R. Roy, M. Rusten, A. Fischer, A.D. Ryabov, B. Blumberg, T.J. Collins, *J. Am. Chem. Soc.* 132 (2010) 9774–9781.
- [17] F.T. De Oliveira, A. Chanda, D. Banerjee, X. Shan, S. Mondal, L. Que Jr., E.L. Bominaar, E. Münck, T.J. Collins, *Science* 315 (2007) 835–838.
- [18] A.B. Sorokin, *Chem. Rev.* 113 (2013) 8152–8191.

[19] S.P. Sun, C.J. Li, J.H. Sun, S.H. Shi, M.H. Fan, Q. Zhou, *J. Hazard. Mater.* 161 (2009) 1052–1057.

[20] T.J. Collins, *Acc. Chem. Res.* 35 (2002) 782–790.

[21] L. Que, W.B. Tolman, *Nature* 455 (2008) 333–340.

[22] G.I. Berglund, G.H. Carlsson, A.T. Smith, H. Szoke, A. Hendriksen, J. Hajdu, *Nature* 417 (2002) 463–468.

[23] J. Rittle, M.T. Green, *Science* 330 (2010) 933–937.

[24] T.J. Reid, M.R. Murthy, A. Sicignano, N. Tanaka, W.D. Musick, M.G. Rossmann, *Proc. Natl. Acad. Sci. USA* 78 (1981) 4767–4771.

[25] A.K. Roy Choudhury, *Textile Preparation and Dyeing*, Science Publishers, Enfield, NH, 2006.

[26] A.A. Mansur, H.S. Mansur, F.P. Ramanery, L.C. Oliveira, P.P. Souza, *Appl. Catal. B: Environ.* 158–159 (2014) 269–279.

[27] R.A. Pereira, M.F.R. Pereira, M.M. Alves, L. Pereira, *Appl. Catal. B: Environ.* 144 (2014) 713–720.

[28] L. Ai, C. Zhang, L. Li, J. Jiang, *Appl. Catal. B: Environ.* 148–149 (2014) 191–200.

[29] C. Tan, G. Zhu, M. Hojamberdiev, K. Okada, J. Liang, X. Luo, P. Liu, Y. Liu, *Appl. Catal. B: Environ.* 152–153 (2014) 425–436.

[30] W. Chen, W. Lu, Y. Yao, M. Xu, *Environ. Sci. Technol.* 41 (2007) 6240–6245.

[31] J. Mathieu-Denoncourt, C.J. Martyniuk, S.R. De Solla, V. Balakrishnan, V.S. Langlois, *Environ. Sci. Technol.* 48 (2014) 2952–2961.

[32] C.M. Carilli, S.J. Barclay, C. Shaw, A.D. Wheatley, C.A. Buckley, *Environ. Technol.* 19 (1998) 1133–1137.

[33] Y. Pan, W. Chen, S. Lu, Y. Zhang, *Dyes Pigments* 66 (2005) 115–121.

[34] M.J. Frisch, G.W. Trucks, H.B. Schlegel, G.E. Scuseria, M.A. Robb, J.R. Cheeseman, G. Scalmani, V. Barone, B. Mennucci, G.A. Petersson, H. Nakatsuji, M. Caricato, X. Li, H.P. Hratchian, A.F. Izmaylov, J. Bloino, G. Zheng, J.L. Sonnenberg, M. Hada, M. Ehara, K. Toyota, R. Fukuda, J. Hasegawa, M. Ishida, T. Nakajima, Y. Honda, O. Kitao, H. Nakai, T. Vreven, J.A. Montgomery, Jr., J. E. Peralta, F. Ogliaro, M. Bearpark, J.J. Heyd, E. Brothers, K.N. Kudin, V.N. Staroverov, R. Kobayashi, J. Normand, K. Raghavachari, A. Rendell, J.C. Burant, S.S. Iyengar, J. Tomasi, M. Cossi, N. Rega, J.M. Millam, M. Klene, J.E. Knox, J.B. Cross, V. Bakken, C. Adamo, J. Jaramillo, R. Gomperts, R.E. Stratmann, O. Yazyev, A.J. Austin, R. Cammi, C. Pomelli, J.W. Ochterski, R.L. Martin, K. Morokuma, V.G. Zakrzewski, G.A. Voth, P. Salvador, J.J. Dannenberg, S. Dapprich, A.D. Daniels, Ö. Farkas, J.B. Foresman, J.V. Ortiz, J. Cioslowski, D.J. Fox, Gaussian 09, Gaussian, Inc., Wallingford CT, 2009.

[35] J.D. Hamlin, D.A.S. Phillips, A. Whiting, *Dyes Pigments* 41 (1999) 137–142.

[36] E. Olkowska, Z. Polkowska, J. Namieśnik, *Chem. Rev.* 111 (2011) 5667–5700.

[37] J. Cai, L. Zhang, S. Liu, Y. Liu, X. Xu, X. Chen, B. Chu, X. Guo, J. Xu, H. Cheng, *Macromolecules* 41 (2008) 9345–9351.

[38] N. Isobe, K. Noguchi, Y. Nishiyama, S. Kimura, M. Wada, S. Kuga, *Cellulose* 20 (2013) 97–103.

[39] J.G. Speight, *Lange's Handbook of Chemistry*, 16th ed., McGraw-Hill, New York, 2005.

[40] P. Afanasiev, E.V. Kudrik, F. Albrieux, V. Briois, O.I. Koifman, A.B. Sorokin, *Chem. Commun.* 48 (2012) 6088–6090.

[41] B. Ramdhanie, J. Telser, A. Caneschi, L.N. Zakharov, A.L. Rheingold, D.P. Goldberg, *J. Am. Chem. Soc.* 126 (2004) 2515–2525.

[42] A. Ghosh, D.A. Mitchell, A. Chanda, A.D. Ryabov, D.L. Popescu, E.C. Upham, G.J. Collins, T.J. Collins, *J. Am. Chem. Soc.* 130 (2008) 15116–15126.

[43] J. Du, Q. Li, W. Li, H. Lin, G. Guo, *Acta Cryst. E* 63 (2007) m2597.

[44] Y. Yu, Y. Wei, R. Broer, R. Sa, K. Wu, *J. Solid State Chem.* 181 (2008) 539–551.

[45] T.M. Cocker, R.E. Bachman, *Chem. Commun.* (10) (1999) 875–876.

[46] A.P. Côté, M.J. Ferguson, K.A. Khan, G.D. Enright, A.D. Kulynych, S.A. Dalrymple, G.K. Shimizu, *Inorg. Chem.* 41 (2002) 287–292.

[47] G. Strukul, *Catalytic Oxidations with Hydrogen Peroxide as Oxidant*, Kluwer, Dordrecht, The Netherlands, 1992.